Storm erosion during the past 2000 years along the north shore of Delaware Bay, USA

Daria L. Nikitina[1]*, Andrew C. Kemp[2], Benjamin P. Horton[3], Christopher H. Vane[4], Orson van de Plassche[5,a], and Simon E. Engelhart[6].

1. Department of Geology and Astronomy, West Chester University, West Chester, PA 19383, USA
2. Department of Earth and Ocean Sciences, Tufts University, Medford, MA 02155, USA
3. Sea Level Research, Institute of Marine and Coastal Sciences, Rutgers, New Brunswick, NJ USA
4. British Geological Survey, Environmental Science Centre, Keyworth, Nottingham, NG12 5GG, UK
5. Department of Marine Biogeology, Faculty of Earth & Life Sciences, Vrije Universiteit Amsterdam, De Boelelaan 1085, 1081 HV Amsterdam, The Netherlands
6. Department of Geosciences, University of Rhode Island, Kingston, RI 02881, USA
* Corresponding author, email: dnikitina@wcupa.edu, tel: 610-436-3103
[a] Deceased.

Abstract

Recent impacts of tropical cyclones and severe storms on the U.S. Atlantic coast brought into focus the need for more extended record of storm activity from different geomorphologic settings. Stratigraphic records from estuarine marshes near Sea Breeze, along the north shore of Delaware Bay, document at least seven depositional sequences consisting of peat and mud couplets and representing dramatic changes in sedimentation regime. Abrupt contacts suggest erosion of salt-marsh peat followed by rapid infilling of accommodation space by tidal mud and salt-marsh sediment. The similar depths of erosional surfaces correlated across 2.5 km suggest a common mechanism and we propose that the erosion was caused by storms. Chronological records of two recent episodes of marsh erosion correlate well with historical tropical cyclones in AD 1903 (sequence 7) and AD 1821 or AD 1788 (sequence 6) that impacted the nearby New Jersey Atlantic coast. Six of the sequences may correlate with overwash fans deposited along the New Jersey Atlantic coast since AD 550. Sequence 5 began to form prior to AD 1665-1696 and could result from the same storm that deposited overwash fans in New Jersey and also Rhode Island in AD 1630-1643 and eroded salt marsh in Connecticut during AD 1640-1670. Sequence 4 may correlate with New Jersey fans deposited between AD 1278-1438. Salt marsh in sequence 3 recovered after erosion by AD 900-1150. Sequence 2 dates to AD 429-966 and could be the result of a prehistoric storm that deposited an overwash fan along the New Jersey coast in AD 558-613. Sequence 1 may correlate with the oldest overwash fan deposited in Brigantine, New Jersey. In Sea Breeze the marsh recovery after the first episode of erosion was completed by AD 426-567, while in Brigantine an overwash fan was colonized by marsh vegetation by AD 558-673.

Key words: salt-marsh erosion, tropical cyclones, overwash fan, marsh recovery, Delaware estuary

1. Introduction

The U.S. Atlantic coast is at risk from landfalling tropical cyclones and storms that cause economic, social and environmental devastation. Significant uncertainty surrounds projected tropical cyclone activity in response to climate change (Bengtsson et al., 2007; Emanuel et al., 2008; Knutson et al., 2010). Instrumental and observational records are too short to adequately describe trends in tropical cyclone activity prior to anthropogenic climate change particularly for the largest and rarest events (Elsner, 2007; Landsea, 2007; Liu, 2007). Paleotempestology seeks to reconstruct and explain the spatial and temporal variability in frequency and intensity of landfalling tropical cyclones and severe storms during past centuries and millennia.

Tropical cyclone deposits are most commonly recognized as anomalous sand layers deposited by storm surges in low-energy environments (such as back-barrier marshes, lakes and lagoons) where "normal" conditions between tropical cyclones are characterized by deposition of organic and fine-grained sediments (Donnelly et al., 2001a; Donnelly et al., 2001b; Liu and Fearn, 1993; Madsen et al., 2009; Williams and Flanagan, 2009; Woodruff et al., 2008). The character of these storm-surge deposits varies by locality depending upon the source of sediment, flow characteristics and duration of the storm surge, and local topography (Cahoon, 2006; Hawkes and Horton, 2012; Morgan et al., 1958; Sallenger et al., 2006). Storm surges of sufficient height overtop barrier islands and redistribute sediment from the beach and shore front to the back barrier where it is deposited as a washover fan, often on top of a back-barrier salt marsh. Studies of back-barrier sediments in southern New Jersey revealed that the timing of recent washover fans was consistent with deposition during intense historical storms in AD 1938, AD 1944, AD 1950 and AD 1962 (Donnelly et al., 2001b; Donnelly and Webb III, 2004). Additional overwash deposits were likely deposited by intense tropical cyclones or storms that made landfall in 1821 AD (Donnelly et al., 2001b), 550 to 1400 AD and 500 to 600 AD (Donnelly et al., 2001b;

69 Donnelly and Webb III, 2004). Although the identification of tropical cyclone deposits in coastal
70 lakes and marshes is usually based on the recognition of sand units and/or microfossil evidence,
71 organic geochemical signatures such as C/N, $\delta^{13}C$ and $\delta^{15}N$ provide a complementary approach
72 (Lambert et al., 2008).
73
74 The sedimentary record beneath salt marshes may also preserve an erosive signature of tropical
75 cyclones and storms. For example, lithostratigraphic and radiocarbon data from a Connecticut salt
76 marsh showed widespread erosion events at 1400 to 1440 AD and prior to 1640 to 1670 AD (van
77 de Plassche et al., 2006; van de Plassche et al., 2004). Each time the erosion was followed by
78 rapid and complete infilling of the accommodation space created by erosion with a regressive
79 relative sea-level (RSL) sequence of tidal mud overlain by low-marsh and then high-marsh peat
80 as the salt marsh recovered (Figure 1). The erosive events in Connecticut occurred at the same
81 time as deposition of overwash fans ~60 km away in Rhode Island (Donnelly et al., 2001a). van
82 de Plassche et al. (2006) concluded that the most likely cause of this sedimentary pattern was the
83 erosive action of a storm surge.
84
85 We reconstruct a history of erosional events impacting the northern shore of Delaware Bay in the
86 last ~2000 years by applying the approach of (van de Plassche et al., 2006). Detailed litho-, bio-
87 and chrono-stratigraphic investigation of a salt marsh at Sea Breeze, New Jersey identifies at least
88 seven episodes of substantial erosion followed by marsh recovery. We propose that the erosion
89 was caused by storm surges. This study aids the building of regional databases of past tropical
90 cyclones and/or severe storms that are necessary for comprehensive spatial and time-series
91 analyses.
92

2. Study area

Sea Breeze is located in New Jersey on the northern shore of the Delaware Bay (Figure 2a) and has experienced relative sea level (RSL) rise throughout the Holocene (Engelhart and Horton, 2012; Horton et al., 2013; Miller et al., 2009). From 0 AD to 1900 AD, RSL rose at a rate of ~1.3 mm/yr, which is almost all due to glacial isostatic adjustment (Engelhart et al., 2011). This continuous RSL rise created accommodation space that was infilled by estuarine sediments to preserve a detailed record of relative sea-level change and coastal processes during the Holocene. The region has a semidiurnal, microtidal regime, and the great diurnal range at the nearest NOAA tide gauge is 1.78 m (Reedy Point; Figure 2a). Fine-grained, minerogenic sediments transported by the Delaware River are trapped in the estuary and distributed to the estuarine marshes by tides (Sommerfield and Wong, 2011). Salt marshes on the Delaware Bay (like most on the U.S. Atlantic coast) are highly organic (Nikitina et al., 2003) and include little sand, while silt is the most dominant clastic material.

The Sea Breeze site is a ~2 km wide salt-marsh platform, dissected by tidal channels and underlain by 2-4 meters of salt-marsh and tidal-flat sediments. A paved road runs across the marsh to an abandoned town that existed since late 1800s until 2010. In 2007 Sea Breeze consisted of a single row of 19 houses built between the waterfront and the marsh. A 3-meter-wide man-made channel separated the development from the marsh. To protect homes from storm erosion the state built a sea wall along Beach Avenue. Completed in May 2007 (personal observation) a sea wall was damaged beyond repair by nor'easter in the same year. In 2010 government purchased and knocked down homes and what remains now is remnants of sea wall, a dirt road on infill and the channel. The modern marsh is subdivided into four sub-environments reflecting the varied tolerance of plants to frequency and duration of inundation. Tidal flat environments below mean tide level (MTL) are not colonized by vascular plants and are

characterized by grey mud. Low-marsh environments along the banks of tidal channels correspond to elevations between approximately mean high water (MHW) and MTL and are colonized by tall form of *Spartina alterniflora*. Most of the modern marsh platform is vegetated by *Spartina patens*, *Distichlis spicata* and the stunted form of *Spartina alterniflora*. This high-marsh community typically exists between MHW and mean higher high water (MHHW) (Mckee and Patrick, 1988; Oertel and Woo, 1994). *Phragmites australis* and *Iva frutescens* occupy the elevated banks (levees) of tidal creeks and the borders between salt marshes and freshwater uplands at elevations above MHHW. Meadows of *Schoenoplectus* spp. are also found at the boundary between upland salt marshes and freshwater uplands and represent brackish, waterlogged conditions (Stuckey and Gould, 2000; Tiner, 1985). Macrofossils of plant species from each of the vegetated sub-environments are commonly recognizable in buried sediments and aid reconstruction of tidal flat and marsh facies.

3. Methods

3.1 Core recovery and sampling

The sediment beneath the Sea Breeze salt marsh was described from more than 200 hand-driven gouge cores positioned along seven transects (Figure 2b). Cores were recovered in 1 meter segments with 2.5-cm-wide Eijelkamp core auger (Figure 3a). To insure core quality, multiple cores were taken at sites where gouge was not fully filled with sediment or any signs of sediment disturbance were noticed. Cores were described in the field by sediment type, color, texture, organic content, the presence of identifiable plant macrofossils, and the character of transitions between lithologic units. In an attempt to achieve a full recovery, sediment cores with high moist content were collected in 0.5 m long segments with 0.1 m overlap using 5-cm-wide Russian-type

hand auger (Figure 3b). Selected core sections were photographed to document abrupt changes in lithology (Figure 3ab). We developed a detailed lithostratigraphy from these cores to document sediment accumulation patterns and reconstruct paleoenvironmental changes (Figure 4). We identified plant macrofossils preserved in core material by comparing roots, rhizomes and plant stems preserved with modern examples of the same species and field guides (Niering et al., 1977; Tiner, 1985). Core locations were recorded using GPS and the surface elevation of each core was measured using a Sokkia Total Station and referenced to North American Vertical Datum 1988 (NAVD88). Representative cores for laboratory analysis and dating were recovered in 0.5 m sections using a Russian-type hand auger to minimize compaction due to the coring process, sealed in plastic wrap and refrigerated. One core (number 63, located on transect I-I') was sampled at a resolution of 10cm to ensure that all stratigraphic units were adequately represented. Grain-size and loss on ignition analyses were used to support the documented lithology.

Grain size distribution was measured using a Beckman Coulter laser particle-size analyzer following the sediment preparation procedures of (Pilarczyk et al., 2012). Grain size classifications followed the Wentworth scale. Organic content was determined by loss on ignition (LOI) following the procedures of (Ball, 1964).

3.2 Radiocarbon, ^{137}Cs and stable Pb dating

We sampled identifiable plant macrofossils from six cores (30, 32, 56, 59, 62 and 63) for accelerator mass spectrometer (AMS) radiocarbon dating. Since salt-marsh plants have a known relationship to marsh surface, corms (short, vertical, underground plant stem) preserved in growth position were picked from the sediment cores to ensure the accuracy of dating of paleo-marsh surfaces. Samples were cleaned under a microscope to remove contaminating materials, such as adhered sediment or invasive younger roots, and dried at 50^{o}C. Radiocarbon ages were calibrated using CALIB v6.1.0. (Stuiver and Reimer, 1993) and the IntCal09 calibration data set (Reimer et

166 al., 2011). We report original radiocarbon ages and calibrated years AD/BC with 2σ calibrated
167 uncertainty for fourteen radiocarbon dates (Table 1). The ages constrain when changes in
168 sedimentary environment took place, provide a means to verify correlation of regressive
169 sequences among cores, confirm the presence of erosive hiatuses, and estimate the time necessary
170 for salt-marsh recovery after erosion. The maximum age of erosion was estimated by radiocarbon
171 dating corms of *Spartina alterniflora* found beneath the upper contact of the mud unit that
172 overlies the high-marsh peat (Figure 1f). The minimum age of high salt-marsh recovery was
173 estimated by radiocarbon dating corms of *Spartina patens* and *Schoenoplectus americanus* from
174 the contact between the low-marsh and high-marsh peat (Figure 1e).
175
176 Use of radiocarbon to date macrofossils from the last ~400 years is hindered by a plateau in the
177 calibration curve resulting in multiple ages and large uncertainty. To address this limitation we
178 identified chronostratigraphic markers of ^{137}Cs activity, stable Pb isotopes and Pb concentrations
179 in bulk sediment to constrain recent depositional histories. Three, 80 cm long, cores (24, 30 and
180 56) were recovered with PVC pipe and sampled at 2 cm intervals, dried and ground to
181 homogenized powder (Figure 3c). For measurement of ^{137}Cs activity, samples were sealed in 60
182 ml plastic jars and stored for at least 30 days to ensure equilibrium between Ra and Bi, and then
183 counted for at least 24 h on Canberra Model 2020 low-energy Germanium detectors.
184 Measurements of ^{137}Cs ($t_{½}$ = 30.1 years) activity were made by gamma spectrometry. Peak ^{137}Cs
185 activity occurred in AD 1963 as a result of above-ground testing of nuclear weapons.
186
187 Concentration and isotope ratio determinations for Pb were made using a quadrupole ICP-MS
188 instrument (Agilent 7500c) with a conventional glass concentric nebulizer. The long term 2σ
189 precision for the BCR-2 reference material used for quality control, which has a total Pb
190 concentration of 11 mg/kg was $^{207:206}$Pb = 0.0008, and $^{208:206}$Pb =0.0020, based on *n*=32 replicates

191 over 29 months and a mean accuracy, relative to the published values of (Baker et al., 2004),
192 within that error. Processing consisted of: (i) removal of background; (ii) calculation of isotope
193 ratios; (iii) determination of mass bias correction factor from defined isotope ratios of SRM981;
194 (iv) application of mass bias factors derived from SRM981 using external standard-sample-
195 standard bracketing; and (v) optional further correction for linearity of ratio with signal strength.

196

197 We assumed that most of Pb concentrated in Sea Breeze marsh deposits was transported by
198 prevailing winds from distant industrial centers, rather than from local upstream sources (Graney
199 et al, 1995, Kemp et al, 2012) . Downcore changes in stable Pb concentration identified sediment
200 horizons that correspond to historical changes in U.S. production and consumption. The onset of
201 Pb concentration from background values should correspond to ~ 7-fold increase in national Pb
202 production started in AD 1830 (Kemp et al, 2012). U.S. Pb production peaked at AD 1925 and
203 declined during Great Depression between AD 1930, and AD 1933 (Kemp et al, 2012). A second
204 peak in Pb production and consumption occurred in AD 1974 followed by two-decade decrease
205 due to the phasing out of leaded gasoline (Nriagu, 1998, Kelly et al, 2009). Because residence
206 time of Pb pollutants in the atmosphere is several years and emission values per unit production
207 and consumption is likely changed through time recognized chronological markers are trends
208 rather then absolute values. Changes in the ratio between stable lead isotopes (^{206}Pb:^{207}Pb) were
209 used to establish chronostratigraphic markers from changes in lead production in the Upper
210 Mississippi Valley where lead ores have an unusual isotopic signature (Lima et al., 2005;
211 Marcantonio et al., 2002). Emissions from this region are carried by prevailing winds to the
212 northeastern U.S including New Jersey (Kemp et al., 2012). It is possible to recognize the onset
213 of production in AD 1825, peak production and AD 1857 and the decline of the Upper
214 Mississippi Valley as a significant source of lead production at around AD 1925. The
215 introduction, phasing out, and changing mixture of leaded gasoline enabled recognition of

horizons at AD 1965 and AD 1978 using ^{206}Pb:^{207}Pb profiles.

4. Stratigraphy of Sea Breeze

We recognized six lithostratigraphic units in the sediment underlying the Sea Breeze salt marsh (Figure 5). The depositional environment represented by each unit was determined from organic content and recognizable plant macro-fossils. Grain size analysis indicated a low percentage of sand in the entire system and negligible changes in clay and silt distribution between recognizable units. These six units and associated erosive boundaries were correlated across the site from core logs (Figure 4):

a) The Sea Breeze site is uniformly underlain by pre-Holocene fluvial deposits of gray, fine to medium size sand.
b) This is overlain by a black, humic, sandy mud that we interpret as a paloesol.
c) A dark brown to black basal peat with fragments of *Schoenoplectus* spp., is found in the majority of cores on transects I-I' and II-II' at elevations below -2.5 m NAVD88 (Figure 4). This peat was likely deposited in a brackish environment at the transition between the salt marsh and freshwater upland; similar to the modern transition environment at Sea Breeze. Dated fragments of *Schoenoplectus* spp. in core 32 indicate that brackish tidal marshes began to develop at Sea Breeze around 290BC ± 40 years (Table 1).
d) A gray-brown, fibrous peat overlies the paleosol and brackish marsh deposits. The presence of *Spartina patens* and *Distichlis spicata* macrofossils within this peat indicate that it accumulated in a high-marsh environment between MHW and MHHW.

e) A gray mud described at different stratigraphic levels above high-marsh peat represents tidal deposits. Vertical stems of *Spartina alterniflora* deposited above tidal mud illustrate colonization by low-marsh vegetation.

f) A gray-brown muddy peat with abundant *Spartina alterniflora* fragments was likely deposited in a low-marsh environment.

Following deposition of the high-marsh peat, the stratigraphy at Sea Breeze shows at least seven repeated sequences (numbered 1 to 8, from oldest to youngest) of high salt-marsh peat overlain by gray mud with little (<15%) organic matter, representing tidal-flat deposits, which recovers to a low marsh and then to high-marsh environment (Figure 1). The contacts between the high mash peat and overlying mud are sharp (<1 mm), suggesting an abrupt change in the sedimentation regime and environment of deposition (Figure 3ab, 5).

Sequence 1. A brackish/high-marsh peat is abruptly overlain by a ~10 cm thick gray tidal-flat mud. The upper contact of the mud occurs at ~-2.5 m NAVD 88 (~3.5 m below modern marsh surface) (Figure 4). The mud unit is overlain by gray-brown, low-marsh muddy peat. Rhizomes of *Spartina alterniflora* recovered immediately below the transition between mud and low–marsh, muddy peat in core 63 indicate that the tidal flat was colonized by salt-marsh vegetation between AD 260 and AD 520 (Figure 5). The low-marsh peat is capped by high-marsh peat that accumulated at the elevation of -2.25 m NAVD 88 by AD 429 to AD 567, based on a dated fragment of *Schoenoplectus* spp. (core 59; Transect III). Sequence 1 was complete along transects I, II, and III (Figure 4).

Sequence 2. The high-marsh peat from sequence 1 is abruptly overlain by a 10 to 60 cm thick tidal-flat mud. The upper contact of the mud was documented at the elevation of -2.0 m NAVD 88 (Figure 4). The mud was capped by a low-marsh peat. A *Spartina alterniflora* rhizome in core 63 yielded a maximum age of AD 776 to AD 966 for when low-marsh

plants recolonized the tidal-flat surface. The age of a *Spartina alterniflora* stem found in the overlying high-marsh peat in core 62 indicates that high-marsh vegetation had recolonized by AD 890 to AD 1030 at an elevation of -1.8 m NAVD 88. Sequence 2 was complete along the north-west portion of Transect I (cores 62-78), and at selected sites along II (cores 81, 13, 69, and 66) and III (core 72).

Sequence 3. The high marsh from sequence 2 is overlain by a 10 cm to 40 cm thick tidal-flat mud. This mud unit occurs between -1.6 m and -2.0 m NAVD 88. In transects I, II, and III, the mud unit unconformably overlies mud or low-marsh peat of sequence 2. Salt-marsh recovery and recolonization of the site by low-marsh plants occurred from AD 900 to AD 1150, as indicated by the first appearance of *Spartina alterniflora* vegetation in the low-marsh peat above the mud in cores 32, 56 and 63. A radiocarbon date from core 30 shows a recovery to a high-marsh environment by AD 893 to AD 1012. High-marsh peat accumulation began at the elevation of ~ -1.5 m NAVD 88. Sequence 3 is found in nearly all cores on transects I, II and III. It was also documented in transect VI.

Sequence 4. A tidal-flat mud (10 to 60 cm thick) abruptly overlies the high-marsh peat of sequence 3. The upper contact of mud was documented at ~ -1.05 m NAVD 88. In transects I to IV the abrupt boundary of the mud unconformably extends into the mud unit of sequence 3. The dated *Spartina alterniflora* stem (core 63) and rhizome (core 59) indicate that a community of low-marsh plants recolonized by AD 1319 to AD 1610 (Figure 5). A high-marsh plant community had recolonized by AD 1451 to AD 1632 (core 63) at the elevation of ~ -0.8 m NAVD 88. Sequence 4 is found in all transects except V.

Sequence 5. The high-marsh peat from sequence 4 is overlain by tidal-flat mud of varying thickness (20 cm to 1.0 m). Though the mud lower contact was documented in more than 20 cores and appeared to be sharp, its bottom boundary unconformably overlaps the mud of sequence 4 in transects I, II, IV and VI. The upper contact of mud occurs at ~ -0.5 m NAVD 88. There is no date available to estimate when low-marsh plants recolonized the

tidal-flat surface. A high-marsh plant community had replaced low-marsh vegetation in sequence 5 by AD 1665 to AD 1814 (core 30). Sequence 5 was documented in all transects. However, its occurrence is limited to one or two core sites located next to each other and therefore, its lateral extent is limited to ~ 50 m except in transects IV and VII where it was correlated across ~ 150 m.

Sequence 6. The high-marsh peat of sequence 5 or 4 is overlain by ~ 20 cm of tidal-flat mud. The upper boundary of the mud occurs at 0 m NAVD 88. The age of salt-marsh recovery was estimated based on peaks of ^{206}Pb:^{207}Pb ratios and Pb and Sb bulk concentration measured in core 56 (Figure 6). The minimum ^{206}Pb:^{207}Pb ratios measured at 0.92 cm to 0.94 cm corresponds to the onset of Pb production in the Upper Mississippi Valley in AD 1827 (Figure 6c). High-marsh peat accumulation above the mud infill occurred between AD 1857 and AD 1875 (Figure 6bc). The complete sequence 6 was documented in all transects except for transect III and VI where a changes in deposition from high-marsh peat to low-marsh muddy peat at the elevation of 0 to -0.2 m NAVD 88 may represent an incomplete sequence 6 (cores 73, 72, 59 and 116, Transect III and cores 86, 98 and 110, Transect VI).

Sequence 7. The high-marsh peat of sequences 6, 5 or 4 is overlain by 10 to 40 cm of tidal-flat mud. The upper boundary of the mud unit is at ~0.5 m NAVD88. The timing of mud deposition was estimated using chronological horizons recognized by downcore changes in Pb concentrations, trends in the ratio of stable Pb isotopes and ^{137}Cs activity in Core 56 (Figures 6 and 7). Deposition of the mud unit began between AD 1900 and 1925 and finished between AD 1963 and AD 1980, when a low-marsh plant community colonized the mud flat. An abrupt change between lithologic units indicates rapid shifting in depositional environments, likelihood of erosion and possible sediment mixing and therefor it is not surprising that chronologic data show some discrepancy. In cores 30 and 56, ^{137}Cs activity peaked at 0.28 m NAVD 88 indicating that low-marsh conditions had

316 reestablished by AD 1963. Stable Pb isotope data from Core 63 is in a good agreement
317 with ^{137}Cs chronology, indicating that low-marsh peat began to deposit shortly after AD
318 1965. However, based on Pb concentration data, low-marsh was not established until after
319 AD 1974. The low-marsh peat is commonly capped by modern high marsh, but at some
320 locations on transects III, IV, V, VI and VII, modern low-marsh peat or tidal-flat mud was
321 deposited on top of the sequence at the elevation of ~0.7 m NAVD 88. Sequence 7 is
322 present in all transects.
323 Sequence 8. High-marsh peat or tidal-flat mud of sequence 7 is overlain by 10 to 20 cm mud
324 unit with an upper boundary at ~ 0.7 m NAVD 88. The mud is overlain by low-marsh
325 muddy peat. Based on the depth of maximum ^{137}Cs activity in cores 24, 30 and 56, salt-
326 marsh plants revegetated the mud after AD 1963. Sequence 8 is present in nine cores in
327 transects III, IV, V and VII. The modern salt-marsh vegetation at theses core sites is tall
328 and short from *Spartina alterniflora* with *Spartina patens*.

329 ## *5. Discussion*

330 ### *5.1 Proposed mechanism of salt-marsh erosion*

331 At Sea Breeze, we identified at least seven stratigraphic sequences of peats and muds that have
332 abrupt contacts suggesting erosion and a dramatic change in sedimentation regime. There are a
333 number of processes that could produce these stratigraphic sequences against a background of
334 rising relative sea level including: lateral migration of tidal creeks (Stumpf, 1983); tidal channel
335 network expansion (D'Alpaos et al., 2007), formation of salt pools (Wilson et al., 2009); changes
336 in sediment delivery rates (Kirwan et al., 2011; Mudd, 2011); rapid relative sea-level change
337 (Atwater, 1987; Long et al., 2006); or erosion during storm events and rapid infilling of the newly
338 created accommodation space (van de Plassche et al., 2006; van de Plassche et al., 2004).
339

340 Salt-marsh tidal creeks are believed to be static features that show very little lateral channel
341 migration due to extensive vegetation root structure that supports their banks (Gabet, 1998;
342 Garofalo, 1980; Redfield, 1972). However, mechanisms that cause the destruction of above and
343 below-ground vegetation, such as deposition of dead vegetation on the creek banks and
344 subsequent development of bare banks or wave erosion may lead to bank face erosion and lateral
345 migration, or enlargement of tidal channels (Chen et al., 2012; Lottig and Fox, 2007; Philipp,
346 2005; Stumpf, 1983). In both cases this is a slow process that results in accumulation of
347 regressive stratigraphic sequences with localized channel-shaped mud facies overlain by peat
348 (Allen, 2000; Nikitina et al., 2003).
349
350 In addition to the limited lateral extent of sedimentary sequences of tidal creek migration,
351 historical observations suggest that this process is unlikely responsible for deposition of
352 sequences 7 or 8 at Sea Breeze. These were created in the late 19^{th} to 20^{th} centuries, during a time
353 period for which maps and aerial photos of Sea Breeze are available. The earliest map of the
354 study area (AD 1887) and aerial photos from the 1930s show a poorly developed network of short
355 and narrow tidal channels (Figure 8ab). The spatially restricted nature of tidal creeks indicates
356 that they cannot be responsible for the site-wide changes in sedimentation. But an extensive
357 network of mosquito control ditches created on Sea Breeze marsh between AD 1887 and AD
358 1930 probably changed marsh hydrology and sediment delivery rates over an extensive area.
359 Historical data illustrates the appearance of seven mosquito control ditches that could be
360 responsible for draining small salt pools documented on the AD 1870-1887 map but absent on the
361 AD 1930 image (Figure 8ab). By AD 1963 most of the ditches were filled in, but segments from
362 different ditches became connected and evolved into the network of tidal channels by AD 1981
363 (Figure 8cd). Unfortunately, the absence of good quality aerial photos for AD 1931-1962 did not
364 allow us to establish more precise relationship between ditches infill and time of deposition of
365 Sequence 7 deposition.

366

367 Salt pools are shallow water-filled depressions common on east Atlantic salt marshes
368 (Adamowicz and Roman, 2005; Redfield, 1972; Turner et al., 1997). Some salt pools form on
369 tidal flats and later become surrounded by salt-marsh vegetation, while others form as result of
370 vegetation disturbance on the marsh surface (Wilson et al., 2009). The stratigraphic signature of
371 salt pools often consisting of dark-grey mud overlain by low-marsh peat is similar to the Sea
372 Breeze regressive sequences. If the stratigraphic record is conformable then the unit underlying
373 the salt pool sequence represents the high salt-marsh environment where the pool originally
374 formed. The bottom contact of such sequences may be erosional as a result of sulfate reduction
375 (van Huissteden and van de Plassche, 1998). Salt pools are of limited extent and typically effect
376 only relatively small parts of the modern marsh at any given time causing marsh fragmentation.
377 Infilled salt pools are preserved in stratigraphic record as discrete rather than laterally continuous
378 mud units present in the study area (Boston, 1983; Day et al., 2000; Wilson et al., 2009).
379 However recent remote-sensing assessment of coastal Louisiana report formation of various “salt
380 ponds” after tropical storm impacts on Louisiana marshes (Morton and Barras, 2011). These
381 storm-impacted marsh features vary in size from closely spaced small scours (plucked marshes)
382 to tens and thousands meter long orthogonal-elongated ponds or amorphous pools up to 1500m
383 across (Barras, 2009). Once formed, erosional salt pools can retain in landscape for decades,
384 enlarge in width and increase in depth after repeated storms. The stratigraphic signature of storm-
385 induced salt pool expansion and infill would be synchronous, continuous mud units overlain by
386 organic-rich tidal flat mud and salt marsh peat, similar to Sea Breeze sequences.
387

388 Processes that change relative sea-level rapidly on a local scale include sediment compaction,
389 tidal-range change and, in case of tectonically active coast, earthquakes. (Törnqvist et al., 2008)
390 suggested that compaction of Holocene strata contributes significantly to the exceptionally high
391 rates of relative sea-level rise and coastal wetland loss in the Mississippi Delta. In, southeast

392 England, (Long et al., 2006) suggested that an originally largely planar peat surface was locally
393 lowered in the tidal frame by sediment compaction and subsequently overlain by tidal flat mud. In
394 these studies the stratigraphy differs from Sea Breeze because only one late Holocene
395 transgressive sequence was identified, where the contact was gradual and the overlying mud
396 sequence was several meters thick.
397
398 Hall et al. (2013) showed that tides in Delaware Bay have steadily gotten larger during the late
399 Holocene and thus would not be responsible for the sequences near Sea Breeze. However, during
400 the 20th century the mean tidal range in the upper estuary increased two-fold in association with
401 dredging and wetland modification in the mid-upper estuary that began in AD 1910 (DiLorenzo
402 et al., 1993). Indeed, historical maps and aerial photos of Sea Breeze document that at least two
403 channels were dredged after AD 1930 and suggest that sediment accumulation on marsh surface
404 changed due to anthropogenic factors. The feedback mechanism caused by systematic deepening
405 of the tidal channels would be the increase of tidal discharges, further channel erosion, and
406 increase in suspended sediment concentrations compensated for by sediment accumulation on
407 tidal flats and marshes (Fredericks, 1995). In response, the marsh surface would either
408 accumulate sediment to maintain a stable tidal elevation and support the characteristic plant
409 community, or experienced increasing frequency and duration of tidal flooding resulting in marsh
410 drowning (Orson et al., 1998). Therefore, the dredging may have been responsible for the
411 deposition of the mud in the recent sequences 7 and 8 and its subsequent colonization by marsh
412 vegetation.
413
414 The stratigraphic record from Plum Island estuary in Massachusetts reported by (Kirwan et al.,
415 2011) is similar to the one in the study area, with the exception that only one sequence consisting
416 of a mud unit overlain by low- and high-marsh peat was recorded. Kirwan et al. (2012) suggested
417 that the Massachusetts sequence records the infill of the estuary and lateral progradation of marsh

418 due to increased sediment delivery associated with European settlement and land clearance that
419 mobilized sediment which ultimately was transported and redeposited in estuaries. Later, Preirtes
420 et al. (2012) argued the relationship between stratigraphy and land use change illustrating that
421 existence of salt marsh segments in Plum estuary predate European settlement as well as overall
422 trend of salt marsh expansion rather than loss. Though, the exact mechanism that changed
423 depositional environments in Massachusetts remains unclear, recent anthropogenic impact
424 significantly changed salt marsh landscape along the Atlantic coast. Similarly, estuarine marshes
425 around Delaware Bay have been modified by humans for over 400 years (Philipp, 2005) and thus
426 may be responsible for one of the more recent sequences (i.e., 6,7 or 8).
427
428 While the most recent changes in marsh sedimentology may be related to land-use change and
429 human modification of the marshes, it is difficult to explain changes of a similar magnitude
430 caused by natural factors prior to human settlement rather than impact by major storms. The
431 uniform depth of the upper contacts between mud and low-marsh peat correlated, in most cases,
432 over 2.5 km suggests a common cause for the erosion. Similarly, the gradual change between the
433 low and high-marsh sedimentation documented at the top of each sequence indicates synchronous
434 marsh recovery.
435
436 Erosion of salt-marsh peat caused by strong wave and current action during marsh inundation
437 under the storm surge conditions followed by rapid mud infill of eroded space and subsequent
438 salt-marsh recovery can explain the repeated deposition of regressive sequences during the on-
439 going transgression and presence of erosive contacts (van de Plassche et al., 2006; van de
440 Plassche et al., 2004) (Figure 1). Marsh erosion may occur during the storm or could be a post-
441 storm process triggered by disturbance of vegetation. Numerical modeling and field observations
442 document that temporal disturbance of marsh vegetation led to platform deepening, expansion of
443 tidal creek network, and temporal decrease in marsh accretion rates (Kirwan and Murray, 2008).

444 All of the above processes may be responsible for sequences 1, 2, 3, 4 and 6 at Sea Breeze.
445 During storm surges enhanced by runoff and stream discharge bed shear stress exceeds the shear
446 strength of mud sediments and erosion undercuts plant root causing slumping of banks and
447 deepening of tidal channels beyond their current scale (Stefanon et al., 2010). This process may
448 be responsible for the stratigraphy we describe for sequence 5.
449
450 Significant loss of salt marshes due to wave erosion, inundation and vegetation loss occurred
451 along the coast of Louisiana after the 1995 hurricane season (Day et al., 2007; Feagin et al., 2009;
452 Ravens et al., 2009). Vulnerability of marshes to storm surge and wave erosion depends on the
453 type of vegetation colonizing the marsh surface. (Howes et al., 2010) reported that low salinity
454 salt marshes predominantly vegetated by *Spartina patens* were more susceptible to erosion, while
455 high salinity salt marshes where *Spartina alterniflora* with extensive horizontal rhizomes is the
456 most abundant species remained unchanged during recent tropical cyclone strikes on Louisiana
457 coastal plain. The Sea Breeze stratigraphic sequences document repeated erosion or decrease in
458 the elevation of high or brackish marshes during the last 2000 years. Models predict that once a
459 portion of marsh is disturbed and submerged, it takes hundred of years to fill the accommodation
460 space with sediment to the depths capable of supporting vegetation (Kirwan and Murray, 2008).

461

462 ## *5.1 Sedimentary Record of Storm Erosion*

463 The sedimentary record of salt-marsh erosion from storm surges at Sea Breeze can be correlated
464 with geological records of tropical cyclone overwash in New Jersey (Figure 5). Back-barrier salt
465 marshes at Brigantine and Whale Beach in southern New Jersey preserved six anomalous sand
466 units deposited since AD 550 (Donnelly et al., 2001b; Donnelly and Webb III, 2004) (Figure 2a).
467 The most recent overwash fan was deposited by the Ash Wednesday storm strike in AD 1962 and

historical accounts suggest sand deposition was widespread on back-barrier salt marshes in New Jersey (Stewart, 1962). Although sequence 8 has variable preservations, the mud was revegetated by *Spartina alterniflora* after AD 1963 in core 24 (Figure 7). However, inconclusive stratigraphy and lack of geochronologic markers from other sites do not allow for correlation of most resent mud deposition with any known storms of the 20th century.

Sequence 7 at Sea Breeze represents erosion that took place between AD 1875 and AD 1925 and we propose that it was caused by a tropical cyclone that made landfall in the Delaware Bay in AD 1903 and was the only tropical cyclone of the 20th century to make landfall in New Jersey (Neumann et al., 1993). This could be the same tropical cyclone that deposited overwash at Brigantine in either in AD 1893 or AD 1903 AD (Donnelly and Webb III, 2004). The timing of erosion and subsequent deposition of sequence 6 at Sea Breeze correlates with overwash fans at Brigantine and Whale Beach that were interpreted as having been deposited by either the 1821 or 1788 tropical cyclone (Donnelly et al., 2001b; Donnelly and Webb III, 2004).

If the high marsh at the top of sequence 5 was eroded in AD 1788, the deposition of sequence 5 began prior to AD 1665-1696, which could be associated with the same storm that deposited an overwash fan in Brigantine around AD 1526-1558 or AD 1630-1643 (Donnelly et al., 2001b; Donnelly and Webb III, 2004). The significant thickness of mud unit, unconformities, and its presence at limited sites suggest that sequence 5 likely associated with erosion and subsequent infill of paleo-channels. In comparison with modern drainage network, the stratigraphy in sequence 5 shows oversized width and depth of paleo-tidal creeks, which could be related to channel erosion due to increased discharge under the storm surge. Deposition of sequence 5 and Brigantine overwash fan of AD 1630-1643 could be the result of the same tropical cyclone that eroded salt marsh in Connecticut and deposited overwash fan in Rhode Island in AD 1635 or AD 1638 (van de Plassche et al., 2006).

Radiocarbon dates indicate that overwash fans were deposited at Brigantine and Whale Beach (Donnelly et al., 2001b; Donnelly and Webb III, 2004) between AD 550-1400 and AD 1278-1438 respectively. During this time period we record sequences 2, 3 and 4. Sequence 4 at Sea Breeze includes a 30-60 cm mud unit that was colonized by salt-marsh vegetation by AD 1319-1351 in transects I and AD 1428-1492 in III. Deposition of this sequence could be result of one or more storms. It is possible that marsh erosion documented by the sharp contact in sequence 4 is the result of the same storm that deposited fans along the New Jersey coast and Rhode Island, and eroded the marshes of Connecticut (AD 1400-1440). If the latter, this storm had a regional impact not only along the coast but on sheltered salt marshes (e.g. Sea Breeze, New Jersey and Pattagansett River Marsh, Connecticut). This correlation is rather tentative and should be further tested at other locations given a wide range of dated evens and great distance between the sites. However, the deposition of ~1m thick overwash fan in Brigantine could be the result of an earlier storm as the sand overlays salt-marsh peat that dates back to AD 558-673. Sequence 3 documented in transects I-III was deposited prior to AD 950-1040. The storm that eroded up to 0.6 m of peat and offset deposition of sequence 2 occurred sometime between AD 429 and AD 966.

Deposition of thin lower sand layer in Brigantine may coincide with the earliest erosion event documented in Sea Breeze (sequence 1). Though only ~ 10 cm of mud was deposited, the evidence of hiatus in core 63 indicates that the elevation of paleo-marsh surface was lowered by erosion. The marsh recovery between AD 260-520 resulted in deposition of low-marsh peat while undisturbed brackish conditions persisted along transect I-I' around AD 214-381 (core 30). The marsh recovery was completed by AD 429-567, which correlates well with AD 558-673 age of salt-marsh surface recovered at Brigantine after deposition of the oldest fan.

We interpreted Sea Breeze stratigraphy as an erosive record assuming that only fragments of local depositional history remained preserved in it. Proposed unconformities between mud units, shown in Figure 4, suggest that sequences were destroyed by later storms. We assume that thick units of mud (> 1m) were formed as multiple storms eroded sequences over and over, followed by infilling of accommodation space with mud units that stacked on top of each other (Figure 4: Transect I cores 14, 50, 26, 46; Transect II cores 82, 13, 70, 67; Transect IV cores 96-104). Simultaneous salt pool expansion cause by storm erosion is a plausible explanation of Sea Breeze stratigraphic sequences as well. Nevertheless this record is relevant to paleotempestology as it identifies storm-related deposition and may contribute to building a regional database necessary for comprehensive spatial and time-series analyses of former storm activity.

6. Conclusion

Seven complete plus one incomplete regressive sequences marked by abrupt contacts were documented in salt-marsh deposits in Sea Breeze, NJ. This record of erosive boundaries and mud infilled accommodation spaces correlates well with historical and geological record of tropical cyclone activity and indicates that at least seven tropical cyclones and/or storms have struck the northern shore of Delaware Bay in the past 2000 years. This record compliments and extends the limited geologic data of tropical cyclone erosion for southern New Jersey. It also proves that salt-marsh sedimentary sequences can be used as a tool for storm impact risk assessment. Lateral continuity of erosive boundaries mapped in the study area indicates that estuarine salt marshes are as vulnerable to storm erosion as the ocean coast and provide evidence that severe storms affect by far larger areas than just a shoreline.

7. Acknowledgments

We pay tribute to Orson van de Plassche, whose pioneering work on tropical cyclone erosion of salt marshes in New England paved the way for this study. Funding for this study was provided by NICRR grant DE-FC02-06ER64298, 2007 PASSHE Faculty Development Award and West Chester University of Pennsylvania seed grants. ^{137}Cs dating was conducted by Dr. Christopher Sommerfield, College of Earth, Ocean and Environment, University of Delaware. We thank the enthusiastic help with fieldwork from participants in the Earthwatch Student Challenge Awards Program. This paper is a contribution to IGCP project 588 'Preparing for coastal change' and PALSEA. We thank two anonymous reviewers for comments that greatly improved the quality of the manuscript.

Figure Captions

Figure 1. Proposed model for the development of a sedimentary record of tropical cyclone- or storm-induced erosion in a salt marsh. **(A-B)** Under a regime of rising relative sea level, the salt marsh accumulates sediment to preserves its elevation in the tidal frame. **(C)** The action of a storm surge erodes and removes a portion of the previously undisturbed sedimentary record. The now exposed surface is located at a lower elevation with respect to sea level. **(D-E)** The newly created accommodation space is rapidly infilled, first by intertidal mud and then by low-marsh and high-marsh peat as sediment accumulation raises the elevation of the surface in the tidal frame. The resulting sediment is a regressive sequence of relative sea level change. The erosive surface represents a hiatus in the sedimentary record that can be identified by a sharp contact between sedimentary units and a temporal gap in accumulation.

Figure 2. (A) Location of the study site in New Jersey, USA. Depositional records of past overwash events attributed to tropical cyclones or storms are located at Brigantine and Whale Beach (Donnelly et al., 2001b). **(B)** ransects of cores across the Sea Breeze site were used to describe the stratigraphy underlying the modern salt marsh. The location of cores used in detailed analysis and with reported radiocarbon ages are shown.

Figure 3. Examples of sediment cores recovered using different coring devices. Each photo illustrates abrupt contacts between lithologic units. **(A)** Core recovered with 2.5-cm-wide Eijelkamp core auger. A sharp contact between salt marsh peat and tidal grey mud is at 42 cm mark. **(B)** Segment of core 63 recovered with 5-cm-wide Russian peat auger. The photo shows the entire sequence 1 and an abrupt change between high-marsh peat and grey mud of sequence 2 at 355 cm depth. The core was placed in plastic pipe and sampled in the laboratory for ^{14}C AMS

578 dating, grain-size and LOI analysis. **(C)** Core 30 recovered with PVC pipe and sampled for ^{137}Cs
579 dating.
580 **Figure 4.** Stratigraphic cross-sections from seven transects of exploratory cores described at the
581 Sea Breeze sites. The position of radiocarbon dated samples is shown (open circles) and the
582 regressive sequences are numbered 1-8 in each cross section. All vertical axes are altitude
583 relative to North American Vertical Datum 1988 (NAVD88). Dates are calibrated radiocarbon
584 ages expressed in years AD.
585
586
587 **Figure 5.** Downcore lithology identified based on color, texture and macrofossils; grain size, and
588 organic content estimated by loss on ignition (LOI) in core 63, stratigraphic sequences 1-7.
589 Calibrated radiocarbon ages indicate timing of changes in marsh environment and sedimentation
590 regime. Historical tropical cyclone landfalls and dated overwash fans deposited in southern New
591 Jersey are listed for comparison (from (Donnelly et al., 2001b; Donnelly and Webb III, 2004).
592
593 **Figure 6.** Downcore measurements of Pb concentrations and stable isotopic ratios in Core 56. **(A)**
594 organic content estimated by loss on ignition (LOI); **(B)** Concentration of Pb (closed circles,
595 black line) and Sb (open circles, dashed line), dashed lines marked geo-chronological horizons;
596 **(C)** Measured ratio of ^{206}Pb:^{207}Pb, dashed lines marked geo-chronological horizons; **(D)** Detail of
597 measured ^{206}Pb:^{207}Pb ratio between 0 and 50cm.
598
599 **Figure 7.** Downcore measurements of ^{137}Cs activity in cores 24, 30 and 56. Maximum activity
600 occurred in AD 1963 coincident with the peak in above ground testing of nuclear weapons.
601

602 **Figure 8**. Historical map and aerial photographs of Sea Breeze. **(A)** First topographic map of
603 New Jersey completed 1870-1887 (http://historical.mytopo.com). **(B)** 1930 imagery. **(C)** 1963
604 imagery. (D) 1981 imagery (http://www.state.nj.us).
605
606

607 Table 1. Radiocarbon dates from Sea Breeze, New Jersey

Core # (Seq, #)	Lab number	Sample depth (cm)	Sample elevation (m) NAVD88	Material dated	Radiocarbon age	δ ^{13}C (‰, PDB)	Calibrated	Feature dated
32 (3)	Beta-240760	219-224	-1.24	*Sp. Alterniflora*	810 +/- 40	-11	AD 900 to 920 AD 950 to 1040	Post-erosional recolonization of
32	Beta-240761	396-398	-3.98	*Scirpus americanas*	2240 +/- 40	-24.8	BC 390 to 200	Basal peat
56 (3)	Beta-252034	255	-1.62	*Sp. Alterniflora*	810+/- 40	-13.7	AD 980 to 1060 AD 1080 to 1150	Post-erosional recolonization of
62 (2)	Beta-252035	280	-1.83	*Sp. Alterniflora*	1070 +/- 40	-12.8	AD 890 to 1030	High-marsh reco
63 (1)	Beta-252036	352	-2.59	*Sp. Alterniflora*	1460 +/- 40	-12.8	AD 260 to 290 AD 320 to 440 AD 490 to 520	Post-erosional recolonization of
63 (2)	OS-80664	282	-1.89	*Sp. Alterniflora*	1170 +/- 30	-13.63	AD 776 to 901 AD 917 to 966	Post-erosional recolonization of
63 (3)	OS-80663	258	-1.65	*Sp. Alterniflora*	1010 +/- 25	-12.92	AD 981 to 1045 AD 1097 to 1119 AD 1142 to 1147	Post-erosional recolonization of
63 (4)	OS-80692	190	-0.97	*Sp. Alterniflora*	535 +/- 30	-12.56	AD 1319 to 1351 AD 1390 to 1438	Post-erosional recolonization of
63 (4)	OS-80662	170	-0.77	*Sp.Patens*	365 +/- 25	-11.46	AD 1451 to 1526 AD 1556 to 1632	High-marsh reco
59 (1)	OS-84496	290	-2.25	*Scirpus americanas*	1550 +/-25	-23.22	AD 429 to 567	Brackish marsh r
59 (4)	OS-84495	190	-1.02	*Sp.Alterniflora*	425 +/-25	-13.18	AD 1428 to 1492 AD 1603 to 1610	Post-erosional recolonization of
30	OS-	340	-2.43	*Scirpus*	1760 +/- 25	-24.63	AD 214 to 360	Basal peat

	84497			*americanas*			AD 365 to 381	
30 (3)	OS-	244	-1.47	*Sp.Patens*	1090 +/-25	-13.94	AD 893 to 997	High-marsh reco
	84499						AD 1004 to 1012	
30 (5)	OS-	116		*Sp.Patens*	165 +/- 25	-12.91	AD 1665 to 1696	High-marsh reco
	84498		-0.19				AD 1725 to 1786	
							AD 1792 to 1814	
							AD 1835 to 1877	
							AD 1917 to 1952	

608

609

610 **References**

611 Adamowicz, S. and Roman, C., 2005. New England salt marsh pools: A quantitative analysis of
612 geomorphic and geographic features. Wetlands, 25(2): 279-288.
613 Allen, J.R.L., 2000. Morphodynamics of Holocene salt marshes: a review sketch from the
614 Atlantic and Southern North Sea coasts of Europe. Quaternary Science Reviews, 19(12):
615 1155-1231.
616 Atwater, B.F., 1987. Evidence for great Holocene earthquakes along the outer coast of
617 Washington state. Science, 236(4804): 942-944.
618 Baker, J., Peate, D., Waight, T. and Meyzen, C., 2004. Pb isotopic analysis of standards and
619 samples using a ^{207}Pb-^{204}Pb double spike and thallium to correct for mass bias with a
620 double-focusing MC-ICP-MS. Chemical Geology, 211(3-4): 275-303.
621 Ball, D.F., 1964. Loss-on-ignition as an estimate of organic matter and organic carbon in non-
622 calcareous soils. European Journal of Soil Science, 15(1): 84-92.
623 Bengtsson, L. et al., 2007. How may tropical cyclones change in a warmer climate? Tellus A,
624 59(4): 539-561.
625 Boston, K.G., 1983. The development of salt pans on tidal marshes, with particular reference to
626 south-eastern Australia. Journal of Biogeography, 10(1): 1-10.
627 Cahoon, D.R., 2006. A review of major storm impacts on coastal wetland elevations. Estuaries
628 and Coasts, 29(6): 889-898.
629 Chen, Y., Thompson, C.E.L. and Collins, M.B., 2012. Saltmarsh creek bank stability:
630 biostabilisation and consolidation with depth. Continental Shelf Research, 35: 64-74.
631 D'Alpaos, A. et al., 2007. Spontaneous tidal network formation within a constructed salt marsh:
632 observations and morphodynamic modelling. Geomorphology, 91(3): 186-197.
633 Day, J. et al., 2000. Pattern and process of land loss in the Mississippi Delta: A Spatial and
634 temporal analysis of wetland habitat change. Estuaries, 23(4): 425-438.
635 Day, J.W. et al., 2007. Restoration of the Mississippi Delta: Lessons from Hurricanes Katrina and
636 Rita. Science, 315(5819): 1679-1684.
637 DiLorenzo, J., Huang, P., Thatcher, M.L. and Najarian, T.O., 1993. Dredging impacts on
638 Delaware estuary tides, Estuarine and Coastal Modeling III, pp. 86-104.
639 Donnelly, J.P. et al., 2001a. 700 yr sedimentary record of intense hurricane landfalls in southern
640 New England. Geological Society of America Bulletin, 113(6): 714-727.
641 Donnelly, J.P. et al., 2001b. Sedimentary evidence of intense hurricane strikes from New Jersey.
642 Geology, 29(7): 615-618.
643 Donnelly, J.P. and Webb III, T., 2004. Backbarrier sedimentary records of intense hurricane
644 landfalls in the northeastern United States. In: R.J. Murnane and K.B. Liu (Editors),
645 Hurricanes and Typhoons: Past, Present, and Future. Columbia University Press, New
646 York City, pp. 58-95.
647 Elsner, J.B., 2007. Granger causality and Atlantic hurricanes. Tellus A, 59(4): 476-485.
648 Emanuel, K., Sundararajan, R. and Williams, J., 2008. Hurricanes and Global Warming: Results
649 from Downscaling IPCC AR4 Simulations. Bulletin of the American Meteorological
650 Society, 89(3): 347-367.
651 Engelhart, S.E. and Horton, B.P., 2012. Holocene sea level database for the Atlantic coast of the
652 United States. Quaternary Science Reviews, 54: 12-25.
653 Engelhart, S.E., Peltier, W.R. and Horton, B.P., 2011. Holocene relative sea-level changes and
654 glacial isostatic adjustment of the U.S. Atlantic coast. Geology, 39(8): 751-754.
655 Feagin, R.A. et al., 2009. Does vegetation prevent wave erosion of salt marsh edges? Proceedings
656 of the National Academy of Sciences.
657 Fredericks, C.T., 1995. Stability, shear stress and equilibrium cross-sectional geometry of
658 schelted tidal channels. Journal of Coastal Research, 11(4): 1062-1074.

659 Gabet, E.J., 1998. Lateral migration and bank erosion in a saltmarsh tidal channel in San
660 Francisco Bay, California. Estuaries, 4B: 745-753.
661 Garofalo, D., 1980. The influence of wetland vegetation on tidal stream channel migration and
662 morphology. Estuaries, 3(4): 258-270.
663 Graney, J.R., Halliday, A.N., Keeler, G.J., Nriagu, J.O., Robbins, J.A., Norton, S.A., 1995.
664 Isotopic record of lead pollution in lake sediments from northeastern United States. Geochimica
665 et Cosmochimica Acta 59. 1715-1728.

666 Hall, G.F., Hill, D.F., Horton, B.P., Engelhart, S.E. and Peltier, W.R., 2013. A high-resolution
667 study of tides in the Delaware Bay: Past conditions and future scenarios. Geophysical
668 Research Letters, 40(2): 338-342.
669 Hawkes, A.D. and Horton, B.P., 2012. Sedimentary record of storm deposits from Hurricane Ike,
670 Galveston and San Luis Islands, Texas. Geomorphology, 171-172: 180-189.
671 Horton, B. P. , Engelhart, S.E., Hill, D.F., Kemp, A.C., Nikitina, D., Miller, K.G., and Peltier,
672 W.R. 2013. Influence of tidal-range change and sediment compaction on Holocene
673 relative sea-level change in New Jersey, USA. Journal of Quaternary Science, 28(4): 403-
674 411.
675 Howes, N.C. et al., 2010. Hurricane-induced failure of low salinity wetlands. Proceedings of the
676 National Academy of Sciences.
677 Kemp, A.C., Vane, C.H., Horton, B.P., Engelhart, S.E. and Nikitina, D., 2012. Application of
678 stable carbon isotopes for reconstructing salt-marsh floral zones and relative sea level,
679 New Jersey, USA. Journal of Quaternary Science, 27(4): 404-414.
680 Kelly, A.E., Reuer, M.K., Goodkin, N.F., Boyle, E.A., 2009. Lead concentrations and isotopes in
681 corrals and water near Bermuda, 1780-2000. Earth and Planetary Science Letters, 283:
682 93-100.
683 Kemp, A.C et al, 2012 Quaternary Geochronology, 12: 40-49.
684 Kirwan, M.L. and Murray, A.B., 2008. Tidal marshes as the disequilibrium landscapes: lags
685 between morphology and Holocene sea level change. Geophysical Research Letters, 35:
686 L24401.
687 Kirwan, M.L., Murray, A.B., Donnelly, J.P. and Corbett, D.R., 2011. Rapid wetland expansion
688 during European settlement and its implication for marsh survival under modern
689 sediment delivery rates. Geology, 39(5): 507-510.
690 Knutson, T.R. et al., 2010. Tropical cyclones and climate change. Nature Geoscience, 3(3): 157-
691 163.
692 Lambert, W.J., Aharon, P. and Rodriguez, A., 2008. Catastrophic hurricane history revealed by
693 organic geochemical proxies in coastal lake sediments: a case study of Lake Shelby,
694 Alabama (USA). Journal of Paleolimnology, 39(1): 117-131.
695 Landsea, C.W., 2007. Counting Atlantic tropical cyclones back to 1900. EOS, 88(18): 197-202.
696 Lima, A.L. et al., 2005. High-resolution historical records from Pettaquamscutt River basin
697 sediments: 2. Pb isotopes reveal a potential new stratigraphic marker. Geochimica et
698 Cosmochimica Acta, 69(7): 1813-1824.
699 Liu, K.-b. and Fearn, M.L., 1993. Lake-sediment record of late Holocene hurricane activities
700 from coastal Alabama. Geology, 21(9): 793-796.
701 Liu, K.B., 2007. Paleotempestology, Encyclopedia of Quaternary Science. Elsevier, Oxford, pp.
702 1978-1986.
703 Long, A.J., Waller, M.P. and Stupples, P., 2006. Driving mechanisms of coastal change: Peat
704 compaction and the destruction of late Holocene coastal wetlands. Marine Geology,
705 225(1-4): 63-84.
706 Lottig, N.R. and Fox, J.M., 2007. A potential mechanism for disturbance-mediated channel
707 migration in a southeastern United States salt marsh. Geomorphology, 86(3-4): 525-528.

Madsen, A.T., Duller, G.A.T., Donnelly, J.P., Roberts, H.M. and Wintle, A.G., 2009. A chronology of hurricane landfalls at Little Sippewissett Marsh, Massachusetts, USA, using optical dating. Geomorphology, 109(1-2): 36-45.

Marcantonio, F., Zimmerman, A., Xu, Y. and Canuel, E., 2002. A Pb isotope record of mid-Atlantic US atmospheric Pb emissions in Chesapeake Bay sediments. Marine Chemistry, 77(2-3): 123-132.

Mckee, K.L. and Patrick, W.H., 1988. The relationship of smooth cordgrass (*Spartina alterniflora*) to tidal datums - a review. Estuaries, 11(3): 143-151.

Miller, K.G. et al., 2009. Sea-level rise in New Jersey over the past 5000 years: Implications to anthropogenic changes. Global and Planetary Change, 66(1-2): 10-18.

Morgan, J.P., Nichols, L.G. and Wright, M., 1958. Morphological effects of hurricane Audrey on the Louisiana coast, Louisiana State University, Baton Rouge, LA.

Mudd, S.M., 2011. The life and death of salt marshes in response to anthropogenic disturbance of sediment supply. Geology, 39(5): 511-512.

Neumann, C.J., Jarvinen, B.R., McAdie, C.J. and Elms, J.D., 1993. Tropical cyclones of the North Atlantic Ocean, 1871-1992, NCDC/NHC.

Niering, W.A., Warren, R.S. and Weymouth, C.G., 1977. Our dynamic tidal marshes: vegetation changes as revealed by peat analysis.

Nikitina, D., Pizzuto, J.E., Martin, R.E. and Hippensteel, S.P., 2003. Transgressive valley-fill stratigraphy and sea-level history of the Leipsic River, bombay Hook National Wildlife refuge, Delaware, USA. In: H.C. Olson and R.M. Leckie (Editors), Micorpaleontologic proxies for sea-level change and stratigraphic discontinuities, pp. 51-62.

Nriagu, J.O., 1998. Tales told in Lead. Science, 281(5383): 1622-1623.

Oertel, G.F. and Woo, H.J., 1994. Landscape classification and terminology for marsh in deficit coastal lagoons. Journal of Coastal Research: 919-932.

Orson, R.A., Warren, R.S. and Niering, W.A., 1998. Interpreting sea-level rise and rates of vertical marsh accretion in a southern New England tidal salt marsh. Estuarine, Coastal and Shelf Science, 47(4): 419-429.

Philipp, K.R., 2005. History of Delaware and New Jersey salt marsh restoration sites. Ecological Engineering, 25(3): 214-230.

Pilarczyk, J.E. et al., 2012. Sedimentary and foraminiferal evidence of the 2011 Tohoku-oki tsunami on the Sendai coastal plain, Japan. Sedimentary Geology, 282: 78-89.

Ravens, T.M., Thomas, R.C., Roberts, K.A. and Santschi, P.H., 2009. Causes of salt marsh erosion in Galveston Bay. Journal of Coastal Research, 25: 265-272.

Redfield, A.C., 1972. Development of a New England salt marsh. Ecological Monographs, 42(2): 201-237.

Reimer, P.J. et al., 2011. IntCal09 and Marine09 radiocarbon age calibration curves, 0-50,000 years cal. BP. Radiocarbon, 51(4): 1111-1150.

Sallenger, A.H. et al., 2006. Hurricanes 2004: An overview of their characteristics and coastal change. Estuaries and Coasts, 29(6): 880-888.

Sommerfield, C.K. and Wong, K.-C., 2011. Mechanisms of sediment flux and turbidity maintenance in the Delaware Estuary. Journal of Geophysical Research: Oceans, 116(C1): C01005.

Stefanon, L., Carniello, L., D'Alpaos, A. and Lanzoni, S., 2010. Experimental analysis of tidal network growth and development. Continental Shelf Research, 30(8): 950-962.

Stewart, J.Q., 1962. The great Atlantic Coast Tides of 5 – 8 March 1962. Weatherwise, June: 117-120.

Stuckey, I.H. and Gould, L.L., 2000. Coastal plants from Cape Cod to Cape Canaveral. University of North Carolina Press, Chapel Hill, 305 pp.

Stuiver, M. and Reimer, P.J., 1993. Extended ^{14}C database and revised Calib 3.0 ^{14}C age calibration program. Radiocarbon, 35(1): 215-230.

759 Stumpf, R.P., 1983. The process of sedimentation on the surface of a salt marsh. Estuarine,
760 Coastal and Shelf Science, 17(5): 495-508.
761 Tiner, R.W., 1985. Wetlands of New Jersey, U.S. Fish and Wildlife Service, Newton Corner,
762 MA.
763 Törnqvist, T.E. et al., 2008. Mississippi Delta subsidence primarily caused by compaction of
764 Holocene strata. Nature Geoscience, 1(3): 173-176.
765 Turner, I.L., Coates, B.P. and Acworth, R.I., 1997. Tides, waves and the super-elevation of
766 groundwater at the coast. Journal of Coastal Research, 13(1): 46-60.
767 van de Plassche, O. et al., 2006. Salt-marsh erosion associated with hurricane landfall in southern
768 New England in the fifteenth and seventeenth centuries. Geology, 34(10): 829-832.
769 van de Plassche, O., Wright, A.J., van der Borg, K. and de Jong, A.F.M., 2004. On the erosive
770 trail of a 14th and 15th century hurricane in Connecticut (USA) salt marshes.
771 Radiocarbon, 46(2): 775-784.
772 van Huissteden, J. and van de Plassche, O., 1998. Sulphate reduction as a geomorphological agent
773 in tidal marshes ('Great Marshes' at Barnstable, Cape Cod, USA). Earth Surface
774 Processes and Landforms, 23(3): 223-236.
775 Williams, H.F.L. and Flanagan, W.M., 2009. Contribution of Hurricane Rita storm surge
776 deposition to long-term sedimentation in Louisiana coastal woodlands and marshes.
777 Journal of Coastal Research, 56: 1671-1675.
778 Wilson, K. et al., 2009. Stratigraphic and ecophysical characterizations of salt pools: dynamic
779 landforms of the Webhannet salt marsh, Wells, ME, USA. Estuaries and Coasts, 32(5):
780 855-870.
781 Woodruff, J.D., Donnelly, J.P., Emanuel, K. and Lane, P., 2008. Assessing sedimentary records
782 of paleohurricane activity using modeled hurricane climatology. Geochemistry,
783 Geophysics, Geosystems., 9(9): Q09V10.

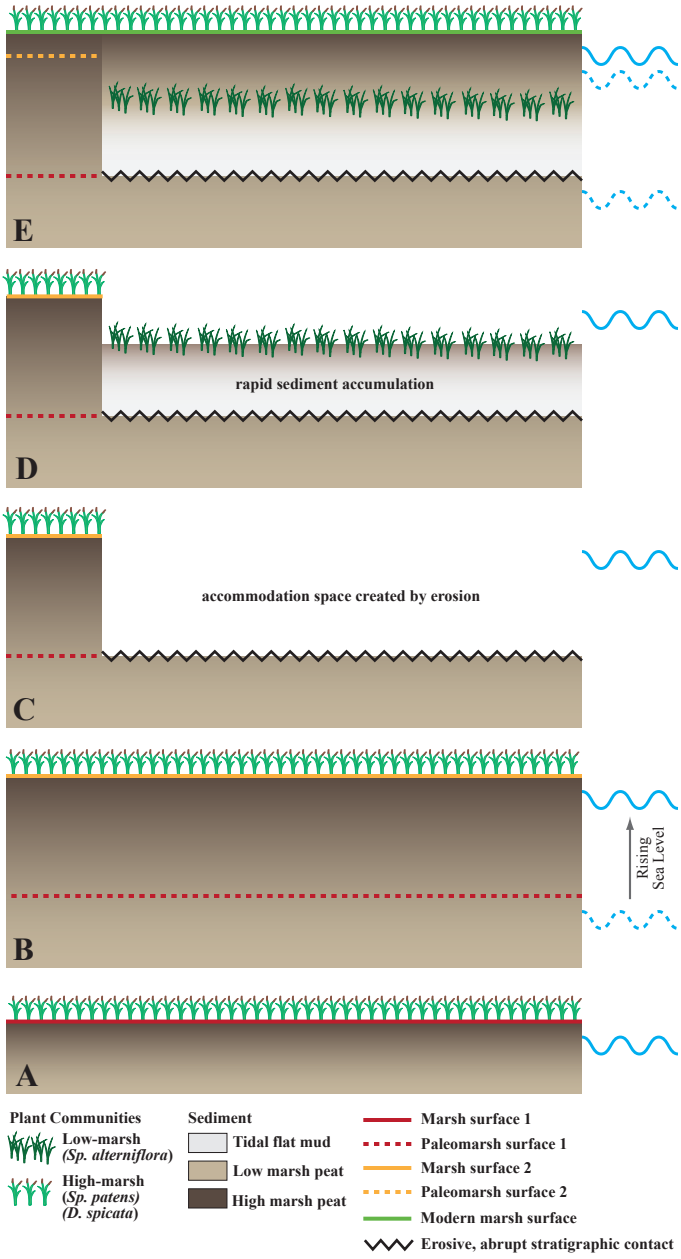
E
rapid sediment accumulation
D
accommodation space created by erosion
C
Rising
Sea Level
B
A
Plant Communities
Low-marsh
(Sp. alterniflora)
High-marsh
(Sp. patens)
(D. spicata)
Sediment
Tidal flat mud
Low marsh peat
High marsh peat
Marsh surface 1
Paleomarsh surface 1
Marsh surface 2
Paleomarsh surface 2
Modern marsh surface
Erosive, abrupt stratigraphic contact

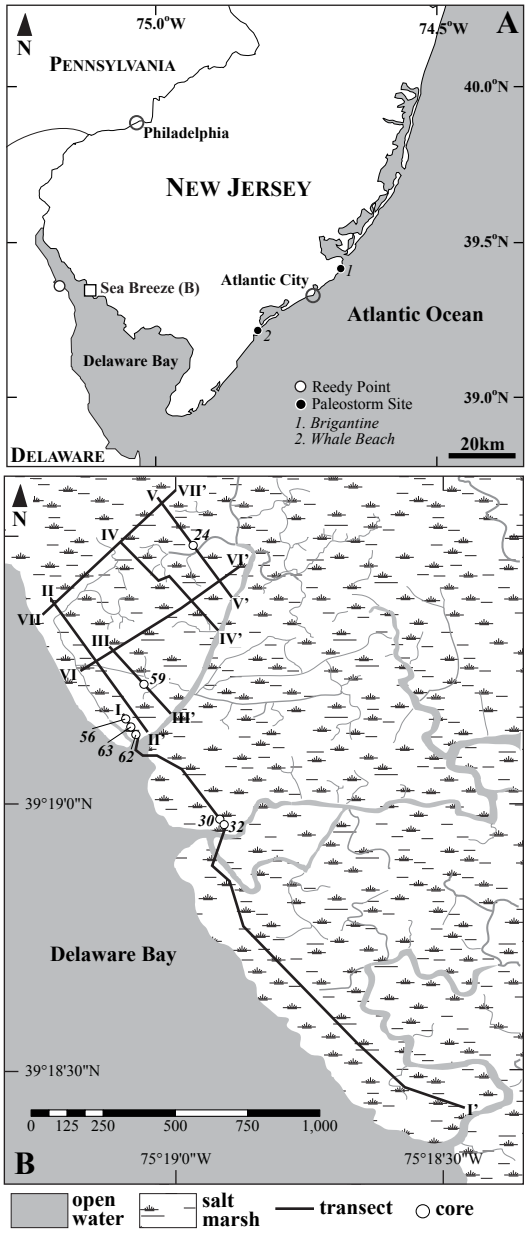
A
N
75.0°W
74.5°W
40.0°N
39.5°N
39.0°N
PENNSYLVANIA
Philadelphia
NEW JERSEY
Atlantic City
Sea Breeze (B)
Atlantic Ocean
Delaware Bay
1
2
Reedy Point
Paleostorm Site
1. Brigantine
2. Whale Beach
20km
DELAWARE
B
N
I
I'
II
II'
III
III'
IV
IV'
V
V'
VI
VI'
VII
VII'
24
59
56
63
62
30
32
39°19'0"N
39°18'30"N
Delaware Bay
0 125 250 500 750 1,000
75°19'0"W
75°18'30"W
open water
salt marsh
transect
core

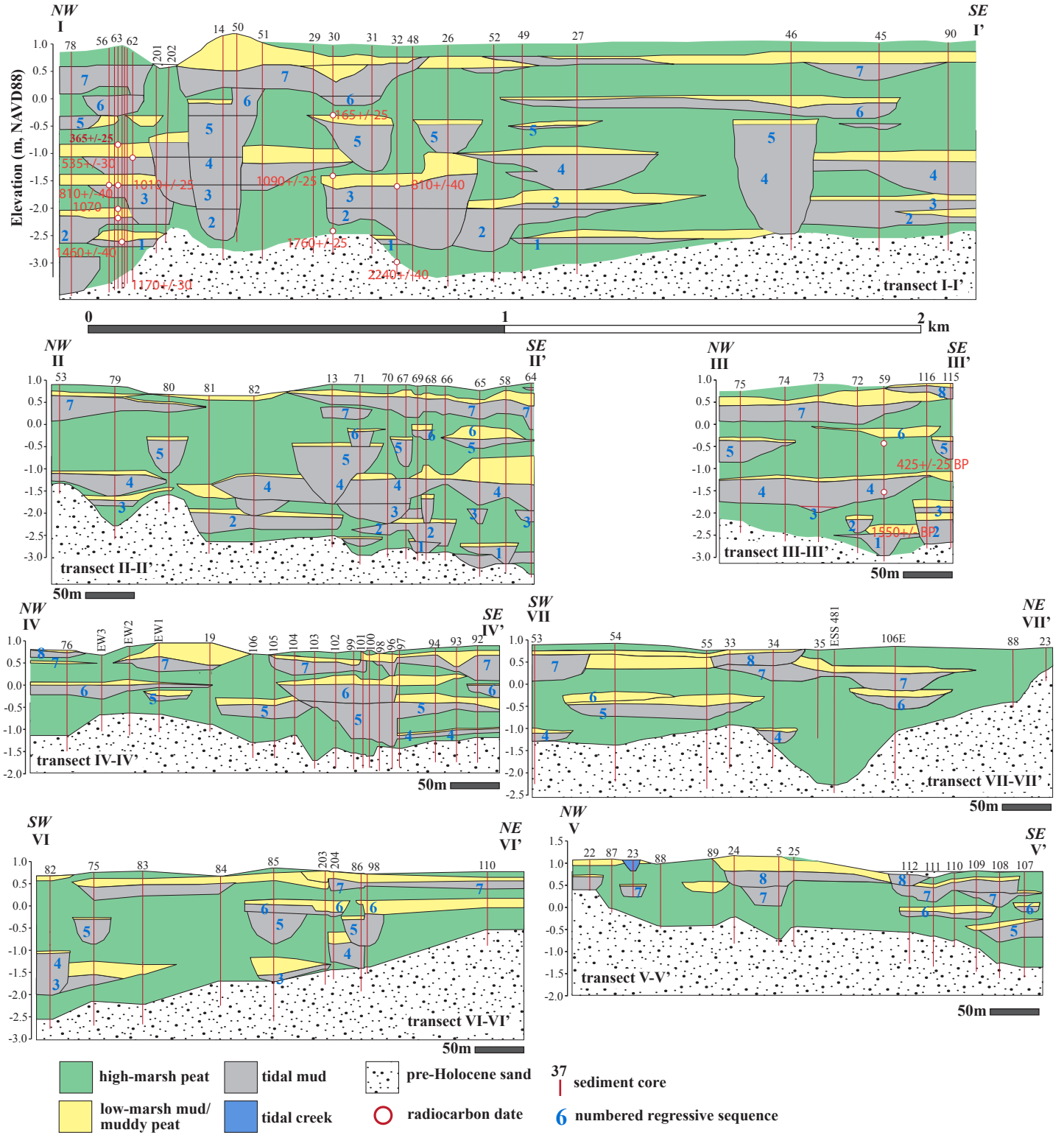
NW
I
SE
I'
Elevation (m, NAVD88)
transect I-I'
0
1
2
km
NW
II
SE
II'
transect II-II'
50m
NW
III
SE
III'
425+/-25 BP
1550+/- BP2
transect III-III'
50m
NW
IV
SE
IV'
transect IV-IV'
50m
SW
VII
NE
VII'
transect VII-VII'
50m
SW
VI
NE
VI'
transect VI-VI'
50m
NW
V
SE
V'
transect V-V'
50m
high-marsh peat
tidal mud
pre-Holocene sand
sediment core
low-marsh mud/
muddy peat
tidal creek
radiocarbon date
numbered regressive sequence

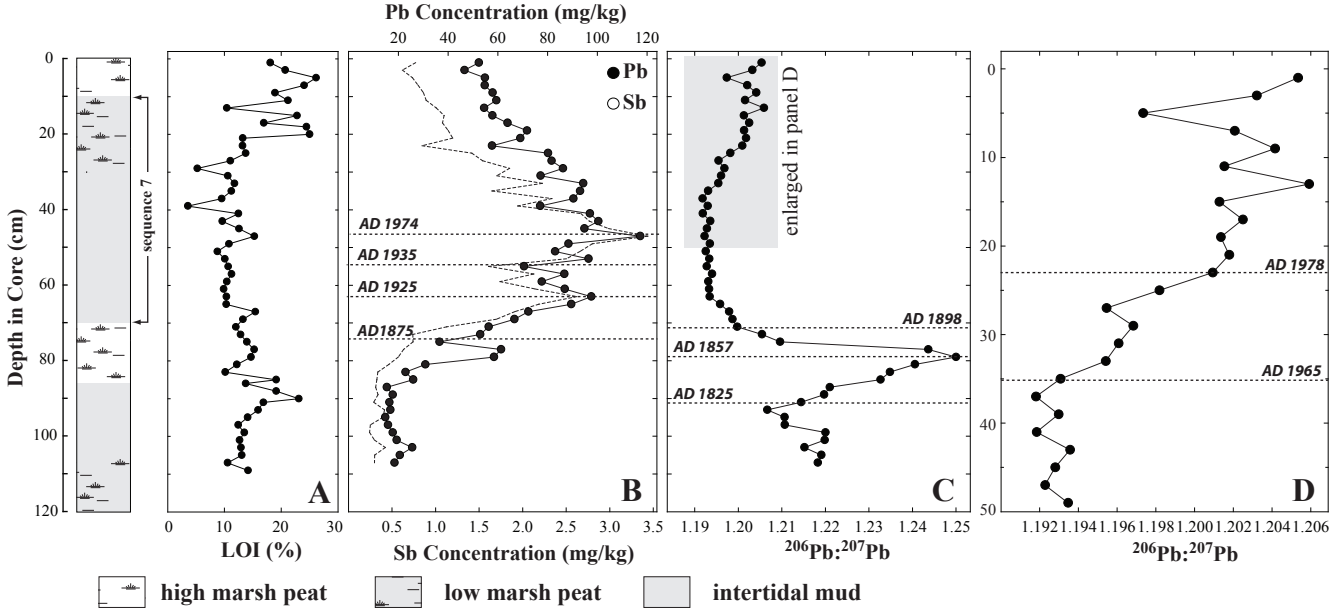
Pb Concentration (mg/kg)
Depth in Core (cm)
sequence 7
LOI (%)
Sb Concentration (mg/kg)
Pb
Sb
AD 1974
AD 1935
AD 1925
AD1875
enlarged in panel D
AD 1898
AD 1857
AD 1825
AD 1978
AD 1965
A
B
C
D
high marsh peat
low marsh peat
intertidal mud

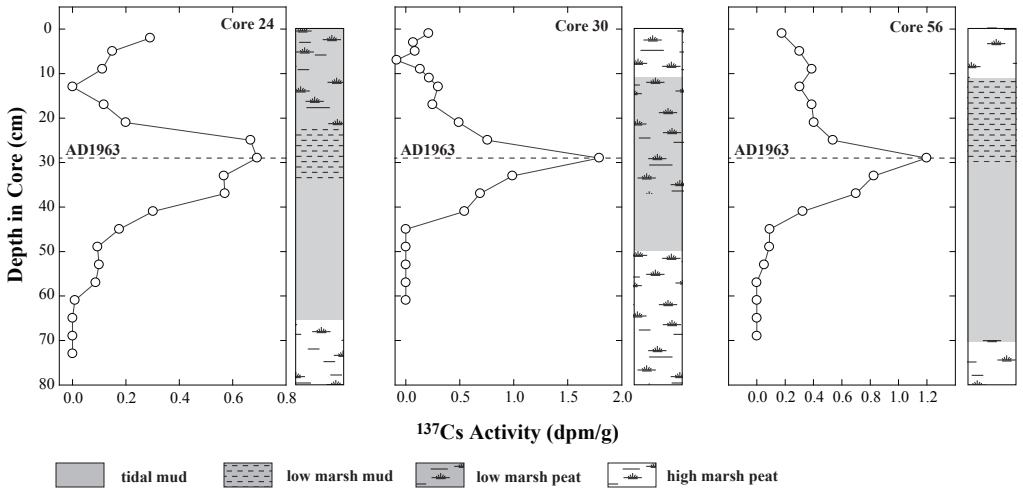
Core 24
Core 30
Core 56
AD1963
AD1963
AD1963
Depth in Core (cm)
0
10
20
30
40
50
60
70
80
0.0 0.2 0.4 0.6 0.8
0.0 0.5 1.0 1.5 2.0
0.0 0.2 0.4 0.6 0.8 1.0 1.2
137Cs Activity (dpm/g)
tidal mud
low marsh mud
low marsh peat
high marsh peat